BULGARIAN ACADEMY OF SCIENCES

CYBERNETICS AND INFORMATION TECHNOLOGIES • Volume **15**, No 7
Special Issue on Information Fusion

Sofia • 2015

Print ISSN: 1311-9702; Online ISSN: 1314-4081
DOI: 10.1515/cait-2015-0089

Fusion of Images Generated by Radiometric and Active Noise SAR

Volodymyr V. Kudriashov[1], *Artem Y. Garbar*[2], *Konstantin A. Lukin*[3], *Lukasz Maslikowski*[4], *Piotr Samczynski*[4], *Krzysztof S. Kulpa*[4]

[1]*Institute of Information and Communication Technologies, BAS, 1113 Sofia, Bulgaria*
[2]*National Technical University "Kharkiv polytechnic institute", 21 Frunze str., 61002 Kharkiv, Ukraine*
[3]*O.Ya. Usikov Institute for Radiophysics and Electronics, National Academy of Sciences of Ukraine, 12 Ak. Proskura str., 61085 Kharkiv, Ukraine*
[4]*Warsaw University of Technology, 15/19 Nowowiejska str., 00-665 Warsaw, Poland*
Emails: KudriashovVladimir@gmail.com Lukin.Konstantin@gmail.com
L.Maslikowski@stud.elka.pw.edu.pl PSamczyn@elka.pw.edu.pl Kulpa@ise.pw.edu.pl

Abstract: *The work is devoted to fusion of radar and radiometer images. Noise waveform SAR generates radar images of reflective objects of its field of view. A bistatic radiometer with synthetic aperture estimates the thermal radio emissions of the objects along their angular coordinates and even range. The estimated brightness temperatures of rough and smooth surfaces are different, as well as the radar responses from them. Identification of the parameters of objects surfaces may be done using results of joint processing of images generated by both sensors. The optimum and quasi-optimum criteria for fusion of the images were obtained. The latter was experimentally checked. It approves the opportunity to fuse the images for further estimation of some parameters of objects surfaces. The results obtained may be used in environmental and security applications.*

Keywords: *Image fusion, microwave radiometer, noise, surface roughness, detection criteria, bistatic radiometer, synthetic aperture radar.*

1. Introduction

Radars achieve requirements towards the electromagnetic compatibility by improved design and enhanced signal processing. Noise radar technology exploits a wideband signal, which is unique from sounding to sounding. The latter assures desired probabilities of interception and exploiting [1, 2]. Fine enough angular

resolution may be achieved using big-sized antennas with mechanic or electronic scanning. Mechanical scanning limits the opportunities to implement sophisticated signal processing and disables graceful degradation of the antenna. The application of phased antenna arrays and multichannel systems leads to significant costs increasing. However, SAR techniques enable to achieve good angular resolution, via moving small antenna and special signal processing. The latter enables avoiding mechanical scanning and decreasing the costs. The noise waveform SAR were built using commercially available components [3, 4]. Such systems provide information on coordinates and reflectivity of objects in the field of view, in the form of a generated image [5, 6]. Each pixel of the image contains phase information along the amplitude one. The phase information enables estimation of objects displacements via differential interferometry technique [7]. The achieved precision of the estimates is better to be 10 μm [8, 9]. It enables to detect pre-catastrophic states of the objects of transport and living infrastructure.

A Bistatic Radiometer (BR) based on antennas with beam synthesis is developed to estimate not only angular coordinates of sources of thermal radio emissions, but their range as well [10-12]. The BR uses the correlation of the incoming signals of the emissions. In addition, the BR generates coherent images. The above approaches enable independent estimation of the objects reflectivity and emissivity. The latter is promising to extract information about the surface (type) of a particular object. Technical opportunity exists to ensure compliance in quality parameters of the images for their joint processing. The possibility of joint estimation of the above objects parameters requires appropriate image fusion technique, which is not available so far.

The object apparent temperature depends on its surface emissivity α [13-15]. The apparent temperature decreases with the increase of both carrier frequency and zenith angle j of the observation. The apparent temperature of an object with smooth surface (calm flat water) equals to 151K for $j = 20°$ [13, 15]. The apparent temperature of object rough surface such as dry grass (asphalt) equals to 263K (238K), for the same angle j. Thus, BR output Signal-to-Noise Ratio (SNR) is in direct ratio to object surface roughness (smoothness).

The surface roughness effects the output SNR of the BR with synthetic aperture, which operates in active mode. At high values of j, the weakest echo-signals are expected in case of mirror reflection of the Noise Waveform Signal (NWS) of illumination. The degree of surface roughness for the mirror reflection can be found from the following equation: $h \le \lambda/(16\cos\phi)$, where h is the height of surface irregularity; λ = 8.17 mm is the wavelength related to the BR carrier frequency [16]. For a zenith angle span from $0°$ up to $30°$, the mirror reflection of NWS can be expected if the roughness height h does not exceed 0.5 mm. Thus, considering the full antenna footprint one may relate to smooth surfaces, such as flat water and window glass. All other surfaces on the generated radiometric image are rough and scatter NWS diffusely.

The work is focused on both the development of optimum and quasi-optimum fusion criteria for radiometric images and images, generated using noise waveform

echo-signals reception, for the same scene and by experimental testing of the developed criterion.

2. Optimum fusion criterion for radiometric and SAR images

Approaches to signal processing in radiometric and radar modes are under consideration for different roughness of objects surfaces. Locus points for equal time difference of arrival comply with a single sheet of the hyperboloid on BR image. Corresponding of the locus points comply with an ellipsoid on image generated using noise waveform echo-signals, in active mode. Both second order surfaces intersect at a right angle. Thus, the fusion of such images can improve the estimation of objects spatial coordinates. The first option of the image fusion is based on an optimum detection criterion of signals with BR. In case of nonmoving objects, the image contains the signal of interest (B=1), otherwise, if the scene has been changed, the image contains no signal (B=0). It is assumed that:

$$P_i(t) = B\,s(t) + n(t), \quad A_i(t) = B\,c(t) + m(t), \quad 0 < t < T, \tag{1}$$

where $P_i(t)$, $A_i(t)$ are signals of pixel i at a radiometric image and image generated using NWS, correspondingly; $s(t)$, $c(t)$ are normally distributed stationary random signals of pixel i at these images; in addition, $s(t)$ and $c(t)$ are correlated when the signal of interest is present; $n(t)$, $m(t)$ are normally distributed non correlated stationary random processes (intrinsic noises of the BR receivers).

It is considered that the width of spectrums of incoming signals has been limited by BR equipment bandwidth Δf and spectral densities of noises $n(t)$, $m(t)$ of its receivers are equal. Introduce a notation: $\overline{s^2(t)} = \sigma_s^2$, $\overline{c^2(t)} = \sigma_c^2$, $\overline{n^2(t)} = \overline{m^2(t)} = \sigma^2$. Under condition $B = 0$, it is obtained: $\overline{P_i^2(t)} = \overline{A_i^2(t)} = \sigma^2$. Under condition $B = 1$ it is obtained:

$$\overline{P_i(t)} = \sigma_p^2 = \sigma_s^2 + \sigma^2, \quad \overline{A_i(t)} = \sigma_a^2 = \sigma_c^2 + \sigma^2,$$

$$\rho_{pa} = \frac{\sigma_s\,\sigma_c}{\left[\left(\sigma_s^2 + \sigma^2\right)\left(\sigma_c^2 + \sigma^2\right)\right]^{0.5}} = \frac{\sigma_s\,\sigma_c}{\sigma_p\,\sigma_a}, \tag{2}$$

where ρ_{pa} is the correlation coefficient for $P_i(t)$ and $A_i(t)$.

According to Kotelnikov theorem, one associates the signals $P_i(t)$ and $A_i(t)$ to vectors of counts $\overrightarrow{P_i} = \{P_1, P_2, \ldots, P_k\}$ and $\overrightarrow{A_i} = \{A_1, A_2, \ldots, A_k\}$. A new vector is constructed as $\overrightarrow{W_i} = \{P_1, A_1, P_2, A_2, \ldots, P_k, A_k\}$. Let us calculate the likelihood ratio, in order to find the optimum criterion [16]. The ratio can be found by means of probability density functions for distribution of $\overrightarrow{W_i}$ parameters for two conditions

(B=0 and B=1). At $B=1$ the $\overrightarrow{W_i}$ parameters are cross-correlated in pairs. Then the joint probability density of the similar samples P_{ij} and A_{ij} submits bivariate normal distribution [16]. Under condition $B=1$, the distribution law $p\left(\overrightarrow{W}/B=1\right)$ for the vector $\overrightarrow{W_i}$ can be found from the above expressions and $p\left(\overrightarrow{W}/B=1\right)=\prod_{j=1}^{k} p\left(P_{ij},\ A_{ij}/B=1\right)$ as follows:

$$p\left(\overrightarrow{W}/B=1\right)=\frac{1}{\left(2\pi\sigma_p\sigma_a\sqrt{1-\rho_{pa}^2}\right)^k}\times \tag{3}$$

$$\times\exp\left[\frac{\sum_{i,j=1}^{k}\left(\sigma_a^2 P_{ij}^2+\sigma_p^2 A_{ij}^2-2\rho_{pa}\sigma_p\sigma_a P_{ij} A_{ij}\right)}{-2\sigma_p^2\sigma_a^2\left(1-\rho_{pa}^2\right)}\right].$$

At $B=0$, all $\overrightarrow{W_i}$ parameters are independent, thus the obtained $p\left(\overrightarrow{W}/B=0\right)$ expression looks like (3), in which the following terms are absent: $\sqrt{1-\rho_{pa}^2}$, $-2\rho_{pa}\sigma_p\sigma_a P_{ij} A_{ij}$ and $1-\rho_{pa}^2$.

The images fusion optimum criterion is found as the maximal value of the likelihood ratio $l\left(\overrightarrow{W}\right)=p\left(\overrightarrow{W}/B=1\right)/p\left(\overrightarrow{W}/B=1\right)$. A logarithm for the likelihood ratio is obtained taking into account $k=2\Delta f\,T$ as

$$\ln\left(\overrightarrow{W}\right)=-\Delta f\,T\ln\left(1-\rho_{pa}^2\right)-\frac{\rho_{pa}^2}{2\left(1-\rho_{pa}^2\right)}\times \tag{4}$$

$$\times\sum_{i,j=1}^{k}\frac{\sigma_a^2 P_{ij}^2+\sigma_p^2 A_{ij}^2-2\sigma_p\sigma_a P_{ij} A_{ij}/\rho_{pa}}{\sigma_p^2\sigma_a^2}.$$

Replacement of the summation by integration enables to express (4) as follows:

$$\ln l\left[P_i(t),A_i(t)\right]=-\Delta f\,T\ln\left(1-\rho_{pa}^2\right)-\frac{\rho_{pa}^2}{2\left(1-\rho_{pa}^2\right)}\times \tag{5}$$

$$\times\int_0^T\frac{\sigma_a^2 P_i^2(t)+\sigma_p^2 A_i^2(t)-2\sigma_p\sigma_a P_i(t)A_i(t)/\rho_{pa}}{\sigma_p^2\sigma_a^2}dt.$$

The first addend in (5) values the threshold for the fused image. The integration weight in the optimum processing procedure (5) equals to $\rho_{pa}^2/2\left(1-\rho_{pa}^2\right)$. Thus, the image fusion optimum processing of a radiometric image and an image, generated using noise waveform echo-signals of illumination source, is obtained as follows:

$$Z \approx \frac{1}{\sigma_p^2 \sigma_a^2} \int_0^T \left[\sigma_a^2 P_i^2(t) + \sigma_p^2 A_i^2(t) - \frac{2\sigma_p \sigma_a P_i(t) A_i(t)}{\rho_{pa}} \right] dt . \quad (6)$$

Rough surfaces (grass, asphalt, etc.), thermal radio emissions and echo-signals enable high values of SNR. The usage of criteria for object surface roughness allows the assumption $\rho_{pa} > 0.5$, which enables simplification (6) to

$$Z \approx \left(\sigma_p^2 \sigma_a^2\right)^{-1} \int_0^T \left[\sigma_a P_i(t) - \sigma_p A_i(t) \right]^2 dt . \quad (7)$$

The first multiplier $\left(\sigma_p^2 \sigma_a^2\right)^{-1}$ of the latter expression shows the pixel-by-pixel normalization of statistically averaged radiometric image σ_p and SAR image σ_a. The sign of integration in the expression changes with a negative value the correlation coefficient ρ_{pa}. The metal objects reradiate the brightness temperature of the cold sky. Echo signals from such objects are significant. Thus, the metal objects present in the field of view can have a negative value of the correlation coefficient ρ_{pa} [16]. The above broadens the opportunities of rough surfaced objects classification on the fused image. A similar effect is expected for smooth conductive objects.

3. Quasi-optimum fusion criterion for radiometric and SAR images

The implementation of the optimum fusion criterion (4)-(6) requires considerable time for the related calculations. So quasi-optimum image fusion criterion is considered for real-time image fusion.

The second variant (heuristic) for the image fusion estimates covariance of the images as given in [16]:

$$\mu_{pa} = \overline{\left(X_p - \overline{X_p}\right)\left(X_a - \overline{X_a}\right)}, \quad (8)$$

where X_p, X_a are normally distributed random signals of each pixel of these images, correspondingly; $\overline{X_p}$, $\overline{X_a}$ are the mean values of each pixel i in these images; μ_{pa} is the covariance of X_p, X_a.

The estimation of X_p, X_a can be performed during signals accumulation. Their mean values $\overline{X_p}$, $\overline{X_a}$ can be calculated in a steady mode of operation (using multiple image realizations, using from 3 to 5 observation time intervals, etc.). The third variant performs valuation of $\overline{X_p}$, $\overline{X_a}$ (8) with a 2D digital filter. The filter comprises a window of 3×3 pixels. The filter calculates the average over the window elements and reassigns the window central element the calculated value. The central element is the filter output signal. Thus, the processing proposed

enables to calculate the covariance matrix μ_{pa} (8) of the images. The correlation coefficient of the random signals X_p and X_a is

$$\rho_{pa} = \mu_{pa} \big/ \left(\sigma_p \, \sigma_a \right), \tag{9}$$

where σ_p, σ_a denote the standard deviation of the random signals at each i pixel of the images for fusion, respectively.

The objects in the image will have a positive value of ρ_{pa}. A negative ρ_{pa} value can be expected from the conductive surfaces of the field of view. Thus, two ways of performing of the fusion of radiometric and SAR images have been considered.

4. Experimental results

The fusion of images, generated experimentally is under consideration. The experiment was carried out in L band. The carrier frequency was 1.25 GHz. Agilent vector signal generator was used as a source of noise signal, generated with third-party software. National Instruments hardware was used as receivers and Analog-to-Digital Converters (ADC) with vertical resolution of 12-bits. The bandwidth was 60 MHz. Coaxial cable Tri-Lan 240 WLL was used for connections. Its wave velocity reduction factor was accounted.

The antennas were mounted on a desk of a multistory building (Fig. 1). Yagi-Uda receiving antennas and transmitting antenna manufactured by Geozondas were used. A trolley with length ~5.3 m was used to perform the step-like shifting of the receiving antenna for aperture synthesis, at left position (Fig. 1a). The second receiving antenna was fixed at right position. The baseline between these antennas was up to ~12.4 m. The transmitting antenna was fixed as well, at right position. The desk dimensions limited the baseline of the noise waveform SAR by ~14.4 m. The trolley motion decreased both baselines. The field of view (Fig. 1b) contained a building, parallel to the cross-range axis, trees and a parking with groups of cars (under the trees). The building range was about 80 m. The experiment used the desk and the listed equipment of department of Prof. K.S. Kulpa, Warsaw University of Technology.

(a) (b)

Fig. 1. The experiment description: The antenna on the trolley (a); the field of view (b)

The bistatic noise waveform SAR enabled to generate an image in range – cross range coordinates. Images for further fusion were generated using straightforward imaging approaches. The normalized image has a color scheme from 0 dB up to –70 dB. The image contains response, which corresponds to the position of the building (Fig. 2). The response is higher than the image background not less than 3 dB.

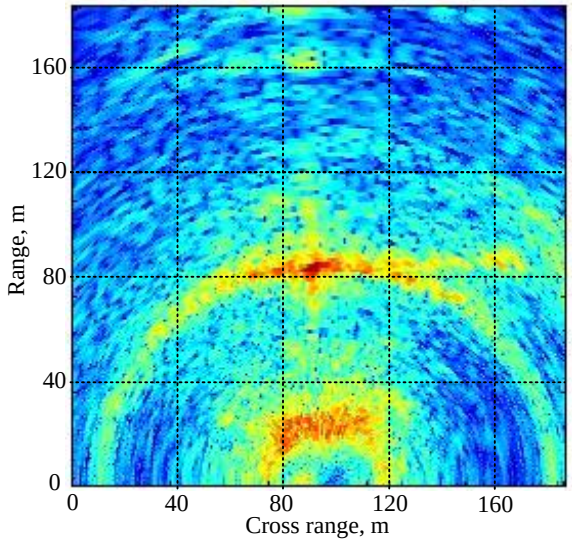

Fig. 2. The image, generated by a bistatic noise waveform SAR

The fusion of the generated images was carried out according to (9), that differs from the optimum one (5), (6). Some pixels of the fused image obtained as pixel-by-pixel estimation of ρ_{pa} correspond to positions of groups of cars (Fig. 3).

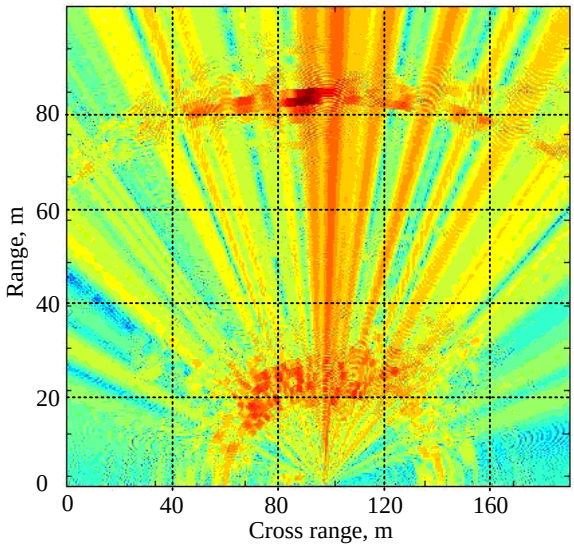

Fig. 3. The image fusion result

The baseline between the receiving antennas is much lower than the range of the targets in the field of view. Thus, the generated radiometric image delivers angular resolution, mainly. The latter limits the quality of the fused image (Fig. 3). The obtained experimental result proves the opportunity of a fuse image generated by a bistatic radiometer with a synthetic aperture to an image, generated by noise waveform SAR. The pixels with negative values of the correlation coefficient correspond to reflections from the sky. Thus, the obtained result is useful for further study on the identification of objects that ensure a negative correlation coefficient.

5. Conclusions

The fusion criteria for the radiometric image and the radar image were developed using surface roughness criteria, for non-shifted field of view. The optimum criterion for the fusion was established, as well as the corresponding threshold level and integration weight. Quasi-optimum criteria for the fusion were presented. The latter enable estimation of the parameters of objects surfaces by means of the covariance matrix or correlation coefficients. Generation and fusion of images with radiometric and noise waveform SAR were provided experimentally. The fusion of the images enables the estimation of emissivity and reflectivity of various objects in the field of view.

***Acknowledgments*:** The research work reported in the paper was partlially supported by Project AComIn "Advanced Computing for Innovation", Grant 316087, funded by FP7 Capacity Programme (Research Potential of Convergence Regions) and by FP-7 Project SCOUT (Grant 607019).

References

1. Kulpa, K., K. Lukin, W. Miceli, T. Thayaparan. Signal Processing in Noise Radar Technology [Editorial]. – Radar, Sonar & Navigation, IET, Vol. **2**, 2008, Issue 4, pp. 229-232.
2. Lukin, K. A., A. G. Stove, K. Kulpa, D. Calugi, V. P. Palamarchuk, P. L. Vyplavin. Ka-Band Ground-Based Noise SAR Trials in Various Conditions. – Applied Radio Electronics, Vol. **12**, 2013, No 1, pp. 145-151.
3. Maslikowski, L., C. Contartese, M. Malanowski, K. Kulpa. Preliminary Results of Ground-Based Noise SAR Experiments. – In: Proc. of 8th European Conference Synthetic Aperture Radar (EUSAR), 2010, pp. 1-4.
4. Maslikowski, L., K. Kulpa. Bistatic Quasi-Passive Noise SAR Experiment. – In: Proc. of 11th International Radar Symposium (IRS), 2010, pp. 1-3.
5. Lukin, K. A., A. A. Mogyla, V. P. Palamarchuk, P. L. Vyplavin, O. V. Zemlyaniy, Y. A. Shiyan, M. Zaets. Ka-Band Bistatic Ground-Based Noise Waveform SAR for Short-Range Applications. – Radar, Sonar & Navigation, IET, Vol. **2**, 2008, Issue 4, pp. 233-243.
6. Tarchi, D., K. Lukin, J. Fortuny-Guasch, A. Mogyla, P. Vyplavin, A. Sieber. SAR Imaging with Noise Radar. – IEEE Transactions Aerospace and Electronic Systems, Vol. **46**, 2010, Issue 3, pp. 1214-1225.
7. Lukin, K., A. Mogyla, V. Palamarchuk, P. Vyplavin, E. Kozhan, S. Lukin. Monitoring of St. Sophia Cathedral Interior Using Ka-Band Ground Based Noise Waveform SAR. – In: Proc. of European Radar Conference, 2009, EuRAD'2009, pp. 215-217.

8. L u k i n, K., P. V y p l a v i n, V. P a l a m a r c h u k, V. K u d r i a s h o v, K. K u l p a, Z. G a j o, J. M i s i u r e w i c z, J. K u l p a. Precision of Target Shifts Detection Using Ka-Band Ground Based Noise Waveform SAR. – In: Proc. of 13th International Radar Symposium (IRS), 2012, pp. 475-478.
9. L u k i n, K. A., P. L. V y p l a v i n, V. P. P a l a m a r c h u k, V. V. K u d r i a s h o v, K. K u l p a, Z. G a j o, J. M i s i u r e w i c z, J. K u l p a. Accuracy of Phase Measurements in Noise Radar. – In: Proc. of 15th International Radar Symposium (IRS), 2014, pp. 1-4.
10. K u d r y a s h o v, V. V., K. A. L u k i n, V. P. P a l a m a r c h u k, P. L. V y p l a v i n. Coherent Radiometric Imaging with a Ka-Band Ground-Based Synthetic Aperture Noise Radar. – Telecommunications and Radio Engineering, Vol. **72**, 2013, Issue 8, pp. 699-710.
11. K u d r i a s h o v, V. V., K. A. L u k i n, V. P. P a l a m a r c h u k, P. L. V y p l a v i n. Range-Azimuth Coherent Radiometric Imaging Based on Ka-Band Antenna with Beam Synthesis. – Applied Radio Electronics, Vol. **11**, 2012, No 3, pp. 328-334.
12. L u k i n K. A. Sliding Antennas for Noise Waveform SAR. – Applied Radio Electronics, Vol. **4**, 2005, No 1, pp. 103-106.
13. V. E. Dulevich, Ed. Theoretical Backgrounds of Radiolocation. Moscow, Sov. Radio, 1978 (in Russian).
14. N i k o l a y e v, A. G., S. V. P e r t s o v. Thermal Radar. Moscow, Military Publishing, 1964 (in Russian).
15. M. I. Skolnik, Ed. Radar Handbook. V. 4. Moscow, Sov. Radio, 1978 (in Russian).
16. Ya. D. Shirman, Ed. Theoretical Backgrounds of Radiolocation. Moscow, Sov. Radio, 1970 (in Russian).